



HAL
open science

Diffusion of organic anions in clay-rich mediaeffect of porosity exclusion on retardation

R.H. V. Dagnelie, S. Rasamimanana, V. Blin, J. Radwan, E. Thory, J-C. Robinet, G. Lefevre

► To cite this version:

R.H. V. Dagnelie, S. Rasamimanana, V. Blin, J. Radwan, E. Thory, et al.. Diffusion of organic anions in clay-rich mediaeffect of porosity exclusion on retardation. *Chemosphere*, 2018, 10.1016/j.chemosphere.2018.09.064 . cea-02339780v2

HAL Id: cea-02339780

<https://cea.hal.science/cea-02339780v2>

Submitted on 10 Oct 2023

HAL is a multi-disciplinary open access archive for the deposit and dissemination of scientific research documents, whether they are published or not. The documents may come from teaching and research institutions in France or abroad, or from public or private research centers.

L'archive ouverte pluridisciplinaire **HAL**, est destinée au dépôt et à la diffusion de documents scientifiques de niveau recherche, publiés ou non, émanant des établissements d'enseignement et de recherche français ou étrangers, des laboratoires publics ou privés.

Diffusion of organic anions in clay-rich media:
retardation and effect of anion exclusion

R.V.H. Dagnelie^(a,*), S. Rasamimanana^(a), V. Blin^(a), J. Radwan^(a),
E. Thory^(a), J.-C. Robinet^(b), G. Lefèvre^(c)

^(a)DEN-Service d'Etude du Comportement des Radionucléides (SECR),
CEA, Université Paris-Saclay, F-91191 Gif-sur-Yvette, France

^(b)Andra, R&D Division, parc de la Croix Blanche 92298, Châtenay-Malabry, France

^(c)PSL Research University, Chimie ParisTech-CNRS, Institut de Recherche de Chimie Paris, 11 rue
Pierre et Marie Curie, F-75005 Paris, France

Dagnelie et al., 2018 - Preprint version - Published version available in Chemosphere

* Corresponding author: R.V.H. Dagnelie, romain.dagnelie@cea.fr, Tel: +33 (0)1 69 08 50 41

Highlights

Retarded diffusion of organic anions was studied in Callovo-Oxfordian claystone

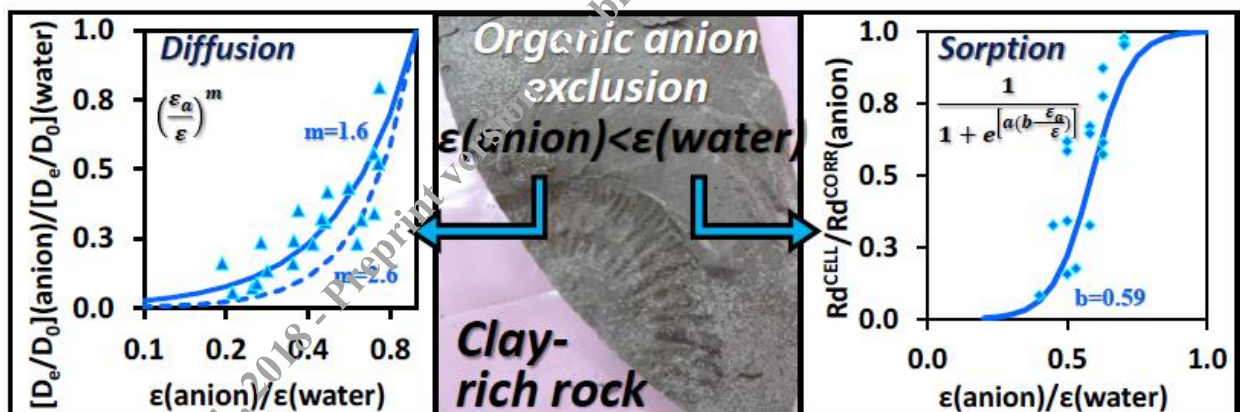
Carboxylates displayed anion exclusion due to both charge and size effects

Anion exclusion lowered accessible porosity and effective diffusion

Diffusive retardation was correlated with hydrophilicity of sorbates

A possible correlation between anion exclusion and retardation is discussed

Graphical Abstract



Abstract

The transport of emerging organic contaminants through the geosphere is often an environmental issue. The sorption of organic compounds slows their transport in soils and porous rocks and retardation is often assessed by extrapolation of batch experiments. However, transport experiments are preferable to strengthen migration data and modelling. In this context, we evaluated the adsorption of various organic acids by means of through-diffusion experiments in a sedimentary clay-rich clay rock (Callovo-Oxfordian, East of Paris Basin, France). A low diffusivity of organic anions was quantified with effective diffusion coefficients, D_e , ranged between 0.5 and $7 \cdot 10^{-12} \text{ m}^2 \text{ s}^{-1}$. These values indicated an organic anion exclusion. As for chloride, the porosity accessible to organic anions was lower than that of water: $\epsilon_a(\text{organic anions}) < \epsilon(\text{water})$. The partial exclusion of organic anions from rock porosity was linked to both charge and size effects. A significant retardation was observed for organic anions such as oxalate, citrate or α -isosaccharinate. Yet, retardation measured by diffusion experiments was significantly lower than expected from batch experiments on crushed samples. An empirical correction factor is proposed to account for a possible decrease of retardation with accessible porosity of diffusing solute. This feature has significant implications for the estimation of migration parameters of organic compounds in the environment.

1. Introduction

Organic pollutants such as anthropogenic organic matter (AOM) can be potentially released from hazardous waste and migrate through geological media or soils (Duarte et al., 2018). AOM refers to a wide range of compounds, with various structures and charges. The ionisable compounds are highly soluble in water and known to be mobile in soils (Schaffer and Licha, 2015). The sorption of organic compounds slows down their migration in environment. In soils, organic ions are preferentially adsorbed on clay minerals and/or oxides (Borisover and Davis, 2015; Gu et al., 1996; Jardine et al., 1989) and neutral organic compounds are often absorbed by soil organic matter (Borisover and Graber, 1997; Curtis et al., 1986; Weber et al., 1991). The migration of organic molecules was mainly investigated in many oxide-rich soils and model materials, e.g. purified clays (Liu et al., 2014). Predicting the migration of organic compounds requires the knowledge of relevant site-specific mechanisms controlling transport, e.g. adsorption-dissociation processes (Szecsody et al., 1998; Zachara et al., 1995), slow sorption kinetics (Brusseau, 1991), colloidal effects (Roy and Dzombak, 1998), etc. In this study, we studied the diffusion of organic anions in clay-rich rocks, for which a complex behaviour was evidenced (Chen et al., 2018; Dagnelie et al., 2014 and 2015; Descostes et al., 2017; Durce et al., 2014).

During the last decade, a significant effort was made to study the migration of solutes through geological media in the context of deep underground radioactive waste disposal (Delage et al., 2010; Tournassat et al., 2015). Various sedimentary clay-rich rocks were investigated, e.g. Callovo-Oxfordian clay rock (COx, France), Boom clays (Belgium), Opalinus clays (Switzerland) (Altman et al., 2012; Charlet et al., 2017). These rocks are characterized by low hydraulic conductivities and low diffusion coefficients due to their narrow pore network. Clay-rich rocks display high retention properties of cations. The adsorption of cations on constituting clay minerals induces significant diffusive retardation (Melkior et al., 2007; Savoye et al., 2012a; 2015). On the contrary, anions are repelled from the surfaces of pores leading to the well-established “anion exclusion” phenomena (Bazer-Bachi et al.,

2007; Descostes et al., 2008; Frasca et al., 2012; Savoye et al., 2012b, Montavon et al., 2014; Wigger and Van Loon, 2017). The behaviour of small organic anions was found to be intermediate between those of cations and inorganic anions (Dagnelie et al., 2014; Descostes et al., 2017). These compounds are studied for various safety assessments, including complexation and transport of metal and radionuclides (Nowack et al., 1997; Read et al., 1998; Hummel, 2008; Charlet et al., 2017). Carboxylates simultaneously undergo “anion exclusion” and sorption. Yet, only few studies have assessed the simultaneous effect of anion exclusion and of retardation (Savoye et al. 2012a; Shackelford and Moore, 2013). In a recent study, Rasamimanana et al. (2017a) quantified the adsorption of various carboxylates on COx clay rock. The solid-liquid distribution coefficients, R_d , ranged from 0.1 to several tens of $L\ kg^{-1}$. Similarly, moderate affinities of carboxylates were confirmed by migration experiments (Chen et al., 2018; Dagnelie et al., 2014; Descostes et al., 2017; Durce et al., 2014).

A key point that remains unclear is the discrepancy between R_d values measured for organic anions by batch and diffusion experiments (Dagnelie et al, 2014; Durce et al. 2014). These observations led to put forward several hypotheses, such as experimental bias due to bacterial activity or oxydoreduction (Rasamimanana et al., 2017b), effect of minor phases (Dagnelie et al., 2015), or effect of anion exclusion on retardation (Van loon et al., 2018). In order to assess these hypotheses, we evaluated the diffusive behaviour of various organic anions in COx clay rock. The results were discussed with emphasis on applicability of adsorption data obtained on crushed rock to the migration modelling in sedimentary rocks.

2. Material and methods

2.1. Rock samples

Experiments were carried out on samples that originated from the Callovo-Oxfordian sedimentary formation (East of Paris Basin, Meuse/Haute-Marne, France). The rock cores, EST40471, EST207_16509, EST207_16517 and EST207_16520, were drilled from a borehole in the underground

laboratory at -501 m and -498 m in depth. The samples come from the clayey unit constituted by 50-55% of clay minerals (illite, interlayered illite-smectite, kaolinite, chlorite), 18-20% of tectosilicates (mainly quartz), 22-35% of carbonates (mainly calcite, dolomite), < 5% of accessory minerals (pyrite, iron oxide...) and ~ 0.6% of organic matter (Gaucher et al., 2004; Lerouge et al., 2011; Pellenard and Deconinck, 2014). After drilling, the core samples were protected from oxygen using container under $N_{2(g)}$. Furtherly, the rock cores were sliced inside a glovebox using a wire saw, into samples of a thickness ~10 mm and a diameter ~ 35-40 mm (metrology of samples detailed in supplementary material, Table S1 and S2). The weighting of solid samples led to an average hydrated density $\rho_h \sim 2.34 \pm 0.06 \text{ g cm}^{-3}$ and a total porosity of $\varepsilon(\text{water}) = 21\%$, assuming a grain density $\rho_g \sim 2.7 \text{ g cm}^{-3}$.

2.2. Diffusion experiments

Two kinds of diffusion setups were used, i.e. a static setup with no circulation of the solutions and a dynamic setup with a circulation system of the solutions. The static setup included a cell in polyether ether ketone (PEEK). Samples were pasted with epoxy resin (Sikadur, Sika, France) between two filterplates in contact with upstream / downstream solutions (see Descostes et al., 2008 for detailed setup). The dynamic setup included a stainless steel cell and a samples in contact with solutions circulating in upstream / downstream reservoirs (see Savoye et al., 2011 for detailed setup). Prior to diffusion experiments, the rock samples were pre-equilibrated by filling both upstream and downstream reservoirs with a synthetic porewater (Composition detailed in Rasamimanana et al., 2017b; Ionic Strength: I.S. = 0.105 M). After 48h to 7 days of contact, the solution of both reservoirs was renewed by fresh porewater, and this step was repeated three times. The concentration of exchangeable cations (Na^+ , K^+ , Ca^{2+} , Mg^{2+} , Sr^{2+}) imposed in solution is supposed constant during the diffusion experiments. This hypothesis might be incorrect in the case of contact of the rock with higher concentration of saline plume (Dagnelie et al., 2017) or organic plumes at higher solid-liquid ratios (Dagnelie et al., 2015).

Diffusion experiments were performed either with reference tracers (deuterated or tritiated water: HDO, HTO), non-sorbing anions ($^{36}\text{Cl}^-$) and ^{14}C -labelled or ^3H -labelled organic compounds. The studied organic compounds and their main properties are listed in Table 1. Upstream solutions with organic compounds were prepared by dissolution of acid or sodic salts (> 99% purity) with synthetic porewater. The pH of upstream solutions was adjusted to 7.2 ± 0.2 by adding concentrated solutions of NaOH or HCl. All the studied acids were negatively charged in these conditions (Table 1). The concentration of organic molecules was controlled by Total Organic Carbon analysis (VarioTOCCube from Elementar) or pH dosage with HCl (basic titrino794 from Metrohm). Finally, all the solutions were bubbled before entering glovebox with $\text{N}_{2(\text{g})}$ with CO_2 partial pressure $P_{\text{CO}_2} = 0.6\%$. Sampling and measurements of solution in upstream and downstream reservoirs are given in supplementary material (p.3).

Table 1. Name and properties of the studied organic acids.

Formula, Molecular Weight (M_w) and Octanol Water distribution coefficient (P_{ow}) correspond to the acidic form (HA). Species are under anionic form in CO_x porewater ($\text{pH} \sim 7.2 \gg \text{pK}_{a1}$)

[1] Hansch et al.,1995, [2] Pinsuwan et al.,1995, [3] Sangster,1989.

Studied species (carboxylate: A^-)	IUPAC Name (carboxylic acid: HA)	Formula (HA)	M_w (g mol^{-1})	pKa	$\text{Log}(P_{ow})^{1,2,3}$	Charge at $\text{pH} \sim 7.2$
Acetate	Ethanoic acid	$\text{C}_2\text{H}_4\text{O}_2$	60.05	4.76	-0.17	Ac^-
Adipate	Hexane-1,6-dioic acid	$\text{C}_6\text{H}_{10}\text{O}_4$	146.14	4.43, 5.42	0.09	Ad^{2-}
ortho-Phthalate	Benzene-1,2-dioic acid	$\text{C}_8\text{H}_6\text{O}_4$	166.14	2.94, 5.43	0.73	Ph^{2-}
Oxalate	Ethanedioic acid	$\text{C}_2\text{H}_2\text{O}_4$	90.03	1.25, 4.14	-0.47	Ox^{2-}
α -Isosaccharinate	(2S,4S)-2,4,5-Trihydroxy-2-(hydroxymethyl)pentanoic acid	$\text{C}_6\text{H}_{12}\text{O}_6$	180.16	4.02	-0.8, -2.6	ISA^-
Citrate	2-Hydroxypropane-1,2,3-tricarboxylic acid	$\text{C}_6\text{H}_8\text{O}_7$	192.12	3.13, 4.76, 6.40	-1.64, -1.72	Cit^{3-}
EDTA	2,2',2'',2'''-(Ethane-1,2-diyl)dinitrilo)tetraacetic acid	$\text{C}_{10}\text{H}_{16}\text{N}_2\text{O}_8$	292.24	0, 1.5, 2, 2.7, 6.2, 10.2	-2.6, -3.86	EDTA^{4-}

The list of diffusion experiments and organic compounds is given in Table 2. Detailed information on diffusion experiments is available in supplementary material (Table S1: activities (Bq) and concentrations (mol L^{-1}) of tracers, volumes and ionic strengths in upstream solutions). Finally, the effect of ionic strength on diffusion was assessed by additional experiments with HTO and $^{36}\text{Cl}^-$ in presence of NaNO_3 (detail in Table S2 and results in Fig. S6).

Sterilization of rock was not performed to avoid perturbation of the system by chemical agents (NaN_3) or radiolysis. Still, to prevent bacterial bias, a filtration of synthetic porewater was performed with $0.22 \mu\text{m}$ nylon filters for Experiments n°7 – 15. Molecules such as o-phthalate or EDTA are known to resist bacterial degradation in environmental conditions (Mika et al., 2011; Rasamimanana et al., 2017b; Wang et al., 2017). The possible occurrence of bacterial artefacts, especially for Isosaccharinate or acetate is discussed furtherly.

2.3. Modelling

Sorption was quantified by a solid-liquid distribution coefficient, noted R_d (L kg^{-1}) and defined by

$$R_d = \frac{C_{ads}}{C_e} \quad (1)$$

where C_{ads} (mol kg^{-1}) is the concentration of adsorbed species per mass of adsorbent, and C_e (mol L^{-1}) the concentration in solution at equilibrium with the solid. Adsorption isotherms, $R_d = f(C_e)$, displayed typical Langmuir-Type shape on COx clay rock (Rasamimanana et al., 2017a). This empirical law was modelled using Eq. (2):

$$R_d(C_e) = \frac{K_L \times Q}{(1 + K_L \times C_e)} \quad (2)$$

with K_L (L mol^{-1}) the affinity constant, and Q (mol kg^{-1}) the maximum sorbed amount. All (K_L , Q) parameters for organic acids on COx clay rock are provided in Rasamimanana et al. (2017a).

The analysis of the through-diffusion experiments were based on Fick's second law:

$$\frac{\partial C}{\partial t} = \frac{D_e}{\varepsilon_a + \rho_g(1-\varepsilon)R_d^{CELL}} \frac{\partial^2 C}{\partial x^2} = \frac{D_e}{\alpha} \frac{\partial^2 C}{\partial x^2} \quad (3)$$

with C representing the tracer concentration (mol m^{-3}), t the time (s), D_e the effective diffusion coefficient ($\text{m}^2 \text{s}^{-1}$), ε and ε_a the total and diffusion accessible porosities, ρ_g the grain density ($\sim 2.7 \text{ kg L}^{-1}$). R_d^{CELL} is a solid-liquid distribution coefficient and α is called the rock capacity factor. The initial conditions were $C(x=0) = C_0$, $C(x \neq 0) = 0$. Fully analytical solution of Eq. (3) was obtained in the Laplace space (Crank, 1975; Moridis, 1998). The downstream flux of tracer, J ($\text{moles m}^{-2} \text{s}^{-1}$) was defined by equation (4):

$$J_{down}(t) = \frac{dn_{down}(t)}{S \times dt} = \frac{V_{down}}{S} \times \lim_{\Delta t \rightarrow 0} \frac{C_{down}(t+\Delta t) - C_{down}(t-\Delta t)}{2\Delta t} \quad (4)$$

where dn_{down} is the quantity of tracer reaching the downstream reservoir (in moles or Bq), per unit of time dt (s), and per sample surface S (m^2), V_{down} (m^3) the downstream volume, Δt the duration between two successive measurements and C_{down} (mol m^{-3}) the downstream cumulative concentration, i.e. experimental data corrected from radioactive decay and sampling. All results were discussed on the basis of a normalised flux of tracer:

$$^{NORM}J_{down}(t) = \frac{L}{C_0} J_{down}(t) \quad (5)$$

with L (m) being the sample width and C_0 (moles m^{-3}) the initial concentration of tracer in upstream reservoir. By using $^{NORM}J_{down}$ ($\text{m}^2 \text{s}^{-1}$), the direct comparison of the experiments was possible, regardless of C_0 or L .

Both parameters D_e and α were adjusted by least-square fitting of normalized cumulative downstream flux with a weighting inversely proportional to the experimental precision. The uncertainties ranges on adjusted parameters were evaluated using the precision of the experimental data (Fig. S1 to S5).

Given the high noise on upstream depletion curves, these data were not used for the parametric adjustment. When unavailable, the values for reference tracers were averaged on other samples: $D_e(\text{water}) = 3.6 \pm 10 \cdot 10^{-11} \text{ m}^2 \text{ s}^{-1}$ and $\varepsilon(\text{water}) = 0.18 \pm 0.2$ for experiment n°1-6.

The mass balance was assessed by comparison between upstream experimental data and modelling. Satisfactory mass balances were obtained for experiments n°2, 3, 5, 7, 8, 12, 13, 14, 15 (Fig. S1-S5). These correct mass balances indicate that bacterial activity is unlikely in the case of acetate, Isosaccharinate, oxalate and citrate. Unsatisfactory mass balances were observed in the case of experiments n°1, 4, 9, 10, 11. This result is possibly due to specific effects (Roberts et al., 1986): slow sorption kinetics, competitive effects, biotic or abiotic oxydoreduction. Such possible artefacts are not affecting the main outcomes of the following discussion.

3. Results

3.1. Diffusion of organic acids in Callovo-Oxfordian clay rock

All raw experimental data are given in supplementary material (Fig. S1-S5). The diffusion of organic anions was illustrated in Fig. 1 showing downstream cumulative concentration and corresponding normalized flux. The fluxes underwent a transitory state before reaching a plateau (Fig. 1). The values of the plateaus were representative of the effective diffusion coefficients, $D_e(\text{orga})$. Almost no transitory state was observed in the case of HTO, acetate of adipate, meaning negligible adsorption. Transitory states up to 100 days were observed for oxalate or ethylenediaminetetraacetate (EDTA), indicating significant adsorption. The D_e and α values adjusted from experimental results were gathered in Table 2. The corresponding D_e values, $D_e(\text{orga}) \sim 10^{-12} \text{ m}^2 \text{ s}^{-1}$, were much lower than that of water ($D_e(\text{water}) \sim 3.0 \pm 1.5 \cdot 10^{-11} \text{ m}^2 \text{ s}^{-1}$). These lower effective diffusion coefficients reflected the phenomenon of anion exclusion, as evidenced in sedimentary rocks with inorganic anions (Descostes et al., 2008; Van Loon and Mibus, 2015).

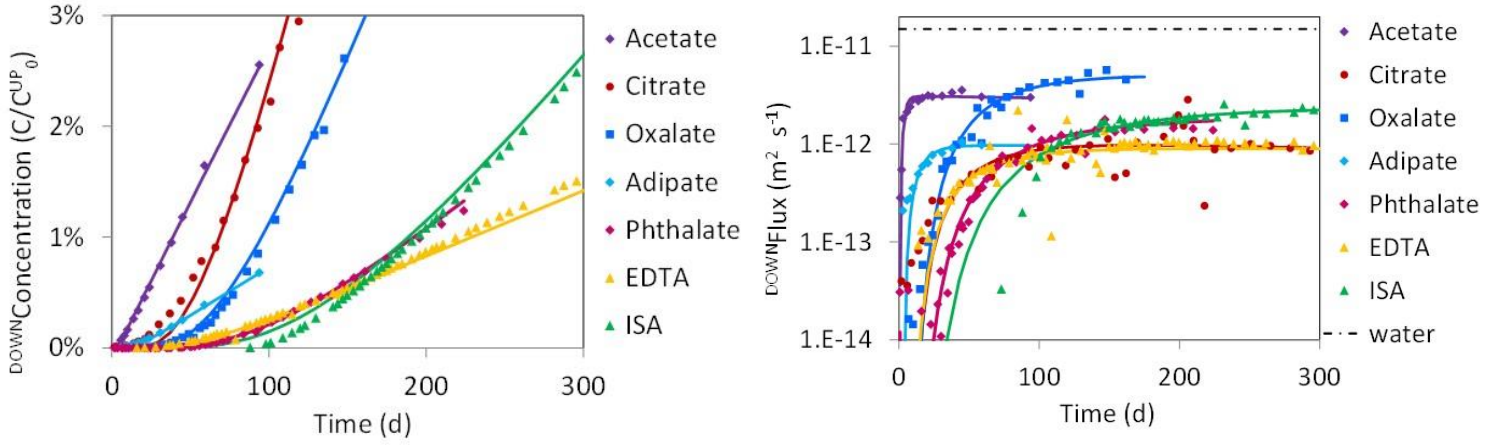


Figure 1: Results from diffusion experiments.

Symbols represent experimental data and solid curves represent best fit modelling. (Left) Downstream concentration normalized by initial upstream concentration. (Right) Normalized downstream flux used for parametric adjustment. (dashed line): Min. value measured for water, $D_e(\text{H}_2\text{O}) = 1.5 \cdot 10^{-11} \text{ m}^2 \text{ s}^{-1}$.

The inter-comparison between experiments using different samples was assessed with the reference tracers (HDO, HTO). A variability by a factor of 3 was observed on diffusivities, with $D_e(\text{HTO})$ ranging from 1.5 to $4.5 \cdot 10^{-11} \text{ m}^2 \text{ s}^{-1}$. Thus, in order to improve accuracy, we normalized diffusion data for anions by the value of the reference tracer. This led to calculate the exclusion factor, Π , defined by the following equation:

$$\Pi = \frac{[D_e(\text{anion})/D_e(\text{reference})]}{[D_0(\text{anion})/D_0(\text{reference})]} \quad (6)$$

where D_e is the effective diffusion coefficient in the porous solid, D_0 the diffusion coefficient in water (I.S. $\sim 0.105 \text{ M}$ and $T \sim 295 \pm 2 \text{ K}$). The diffusing solutes are indicated between brackets: (anion) stands for Cl^- or organic anions and (reference) stands for non-sorbing solutes (HTO or HDO). The ratio $D_e(\text{anion})/D_e(\text{reference})$ quantifies the effect of the saturated clay rock on effective diffusion of anions compared to that of water. The normalization by $D_0(\text{anion})/D_0(\text{reference})$ removes the contribution of the solvent on molecular diffusion. Thus, the ratio Π isolates the effect of electrostatic interactions with surfaces on the diffusion pathway of anions as compared with water (i.e. differences of tortuosity or

constrictivity as defined by Van Brakel and Heertjes (1974)) . For example, a reduced accessible porosity for anions, $\epsilon_a(\text{anion}) < \epsilon(\text{water})$, increases diffusion pathways, e.g. tortuosity and exclusion of anions: $\Pi(\text{anions}) < \Pi(\text{water}) = 1$.

3.2. Anion exclusion in clay-rich rocks: case of chloride

Fig. 2 shows the effective diffusion coefficient and accessible porosities of non-sorbing anion (Cl^-), measured by through-diffusion or percolation experiments on various clay-rich media: COx samples (This work, data in Fig. S6 and Table S2 & S3), compacted Illite (Chen et al., 2018), Opalinus clay and Helvetic Marl (Wigger and van Loon, 2017). In all these studies, a relationship is highlighted between accessible porosities, $\epsilon_a(\text{Cl}^-)/\epsilon(\text{water})$, and ionic strengths. Indeed, the increase of ionic strength reduces the thickness of the diffuse layer at the surface of negatively charged clay minerals, thus decreasing anion exclusion (Van Loon et al., 2007; Wigger and Van Loon, 2017) : i.e. both ϵ_a/ϵ and Π ratios tend to the values for water: $\epsilon_a(\text{water})/\epsilon = 1$ and $\Pi(\text{water}) = 1$ (Fig. 2).

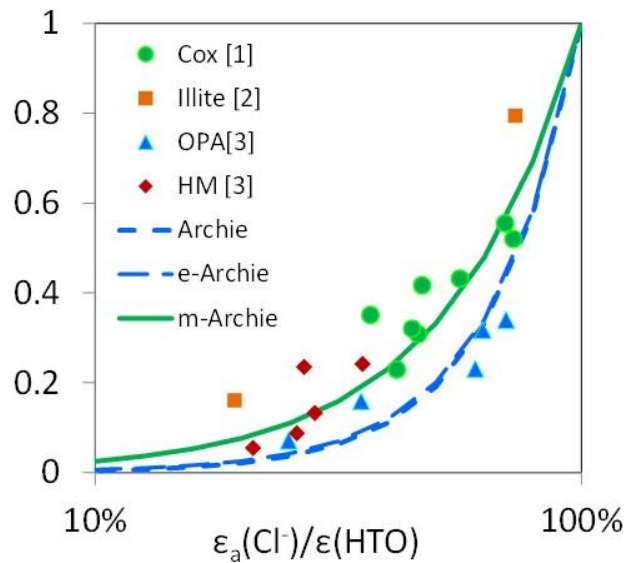


Figure 2: Effect of anion exclusion on the exclusion factor of chloride (Cl^-).

D_e is the effective diffusion coefficient of Cl^- or HTO (tritiated water taken as the reference solute) in COx clay rock. D_0 is the diffusion coefficient in water. [1] Diffusion data in COx (this study). Values between brackets represent ionic strength (in mol L^{-1}). [2] Percolation experiments in compacted illite (Chen et al., 2018). [3] Diffusion experiments in Opalinus Clay (OPA) and Helvetic Marl (HM) (Wigger and Van Loon, 2017). Lines illustrate various empirical laws.

Table 2. Diffusion parameters adjusted from experiments: D_e , ε , α . D_0 values of corresponding carboxylates.

uncertainties between brackets. Calculated data in bold R_d values measured by adsorption on crushed clay (R_d^{BATCH} , Eq. (11)) or diffusion on intact solid (R_d^{CELL} , (Eq. 10)). R_d^{CORR} corrected from porosity exclusion (Eq. (12)). [a] Dagnelie et al., 2014, [b] Descostes et al., 2017, [c] this work, [d] CRC Handbook, 99th Ed. [e] Furukawa et al., 2007 (analogy with Sr-EDTA), [f] Riberiro et al., 2011 (analogy with Ca-Gluconate), [g] (Rasamimanana et al., 2017a).

n°	Tracer	$D_e(\text{water})$ ($10^{-12} \text{ m}^2\text{s}^{-1}$)	$\varepsilon(\text{water})$	$D_0(\text{orga})^{[d]}$ ($10^{-10} \text{ m}^2\text{s}^{-1}$)	$D_e(\text{orga})$ ($10^{-12} \text{ m}^2\text{s}^{-1}$)	$\alpha(\text{orga})$	$\Pi(\text{orga})$	$\varepsilon_a(\text{orga})$	R_d^{CELL} (L kg^{-1})	R_d^{CORR} (L kg^{-1})	$R_d^{\text{BATCH}}^{[g]}$ (L kg^{-1})
1 ^[a]	¹⁴ C-EDTA	36.0	0.18	5.19 ^[e]	0.89 (0.7-1.5)	0.25 (0.21-0.35)	0.12	0.05	0.1	6.5	8.3
2 ^[a]	¹⁴ C- α -ISA	36.0	0.18	8.64 ^[f]	2.97 (2.4-3.7)	2.60 (2.4-2.9)	0.23	0.08	1.1	15.1	13.2
3 ^[a]	¹⁴ C-o-Phthalate	36.0	0.18	6.96	2.50 (1.9-2.7)	0.86 (0.76-0.98)	0.24	0.07	0.4	4.0	1.4
4 ^[a]	¹⁴ C-Oxalate	36.0	0.18	9.87	3.80 (3.6-4.3)	1.37 (1.16-1.8)	0.26	0.08	0.6	5.5	7.9
5 ^[b]	Eu-EDTA	36.0	0.18	5.19	1.36 (0.2-2.0)	3.57 (0.5-4)	0.18	0.06	1.6	43.6	12.5
6 ^[b]	¹⁵² Eu-EDTA	36.0	0.18	5.19	0.45 (0.3-0.6)	1.10 (0.9-1.3)	0.06	0.03	0.5	104.3	12.5
7 ^[c]	¹⁴ C-Oxalate	44.2	0.23	9.87	6.60 (5.5-8.5)	2.74 (2.5-3.5)	0.37	0.12	1.3	4.2	8.4
8 ^[c]	¹⁴ C-Oxalate	37.3	0.23	9.87	6.02 (5.0-6.8)	4.97 (3.8-6.0)	0.40	0.13	2.3	6.2	8.4
9 ^[c]	³ H-o-Phthalate	26.7	0.18	6.96	0.93 (0.7-1.5)	0.07 (0.05-0.08)	0.12	0.05	0.01	0.6	1.5
10 ^[c]	³ H-o-Phthalate	45.1	0.20	6.96	1.28 (0.9-1.7)	0.07 (0.06-0.08)	0.10	0.05	0.01	1.0	1.5
11 ^[c]	³ H-o-Phthalate	25.0	0.13	6.96	0.84 (0.6-1.2)	0.24 (0.22-0.25)	0.12	0.03	0.1	6.0	1.0
12 ^[c]	¹⁴ C-Citrate	18.0	0.15	6.20	1.19 (1.0-1.5)	0.66 (0.45-0.70)	0.26	0.06	0.3	2.5	2.1
13 ^[c]	¹⁴ C-Citrate	22.0	0.18	6.20	1.80 (1.4-2.2)	2.80 (2.6-2.9)	0.32	0.09	1.2	6.1	2.3
14 ^[c]	³ H-Acetate	15.0	0.15	1.09	3.20 (2.9-3.7)	0.07 (0.07-0.12)	0.48	0.10	<0.01	<0.01	<0.1
15 ^[c]	³ H-Adipate	15.0	0.15	6.39	0.98 (0.8-1.3)	0.09 (0.8-0.11)	0.25	0.06	<0.01	0.2	<0.1

A good agreement was observed between diffusion data for chloride and empirical laws. A common model of correlation between diffusion and porosity is provided with the empirical Archie's law, Eq. (7) (Archie, 1942), with parameters $a = 1$ and $m \sim 2.4$. Modified expressions of Archie's law were proposed by several authors for low porosity rocks (Rosanne et al., 2003). Van Loon et al. (2007) proposed a value $m \sim 1.9$ in compacted bentonite with various densities. A modified e-Archie's law was proposed by Van Loon and Mibus (2015) for very low porosity materials ($\varepsilon < 2 \cdot 10^{-2}$). In this study, we will use the specific m-Archie's law evidenced by Jacquier et al. (2013), (Eq. (7) with $a = 0.17$ and $m = 1.6$) for COx samples of variable mineralogy.

$$\frac{D_e}{D_0} = a \times \varepsilon^m \quad (7)$$

$$\Pi(\text{anion}) = \left(\frac{\varepsilon_{a(\text{anion})}}{\varepsilon(\text{reference})} \right)^m \quad (8)$$

Using Eq. (7), the values $D_e/D_0(\text{anion})$ and $D_e/D_0(\text{water})$ were expressed by $\varepsilon_a(\text{anion})$ and $\varepsilon(\text{water})$, in Eq. (6). This led to the correlation between Π and $(\varepsilon_a/\varepsilon)$ defined by Eq. (8) and illustrated in Fig. 2. A good agreement was observed between m-Archie's law and chloride diffusion in COx clay rock, Helevtic Marl, or percolation through compacted illite. This legitimated the use of m-Archie's law with the parameter $m = 1.6$ to compare furtherly our migration results with data from other clay-rich media.

3.3. Anion exclusion in clay-rich rocks: case of organic acids

Fig. 3 shows the exclusion factor of anions, $\Pi(\text{anion})$, measured in COx clay rock (noted $\Pi(\text{orga})$ for organic anions). Low values of exclusion factor were measured for organic anions, $0.1 < \Pi(\text{orga}) < 0.5$, of the same order of magnitude than that of chloride. These values were two to ten times below that of water, $\Pi(\text{water})=1$, illustrating the exclusion of organic anions from a part of rock porosity. Fig. 3 also highlights the correlation of Π with the size of organic solutes, estimated using molecular mass: $M^{-1/3}$.

Firstly, this correlation indicated that a bacterial degradation, leading to small degradation products, was unlikely. Secondly, the dependency between Π and $M^{-1/3}$ indicated that exclusion of organic anions was probably due to both charge and size effects. Large molecule may be more excluded than Chloride from porosity, due to the presence of small pores in clay-rich media (Gaboreau et al., 2016; Wigger et al., 2018). For example, the difference between dianionic species: $\Pi(\text{oxalate}) \sim 0.25-0.36 > \Pi(\text{o-phthalate}) \sim 0.1-0.25$, might be due to a larger size for the later, due to the aromatic cycle (C_6H_5). It was found previously that NO_3^- and Cl^- displayed a similar formal charge but different anion exclusion in COx clay rock (Dagnelie et al., 2017). Thus, the formal charge didn't seem to be a good indicator of anion exclusion (Descostes et al., 2008; Wigger and Van Loon, 2017), but rather charge normalized to the size and polarizability of hydrated organic anion.

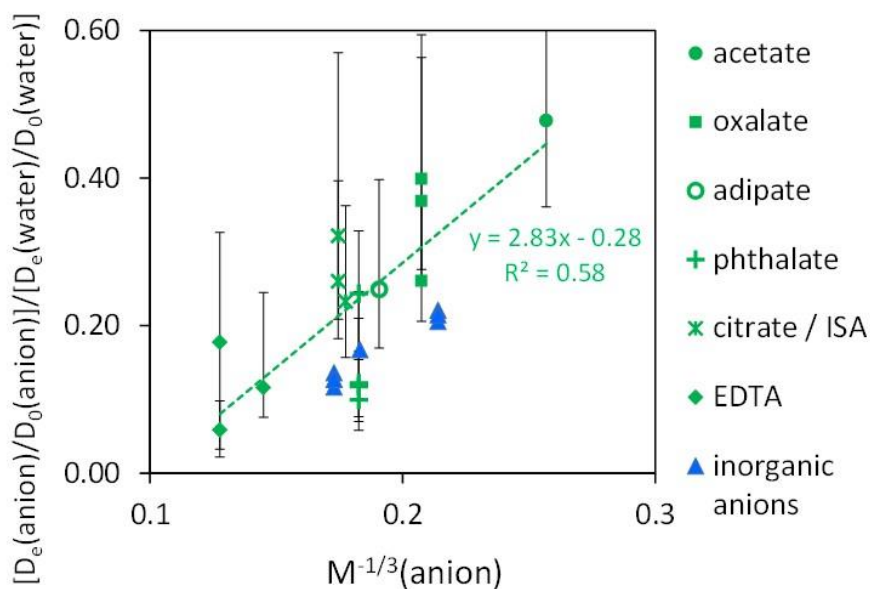


Figure 3: Exclusion factor for organic/inorganic anions in COx clay rock as a function of size.

D_e is the effective diffusion coefficient of solutes in COx clay rock. Water is taken as the reference solute. D_0 is the diffusion coefficient of solutes in water. The size of solutes is estimated using the inverse of molecular mass, $M^{-1/3}$. Dashed line represents the linear regression of values for organic compounds (green symbols). Data for inorganic anions (Cl^- , Br^- , I^- , SO_4^{2-} , NO_3^-) taken from (Bazer-bachi et al., 2006 & 2007; Dagnelie et al., 2017; Descostes et al., 2008; Savoye et al., 2012b).

It was not possible to determine directly accessible porosity of carboxylates. Since adsorption occurs for these compounds, the apparent porosity α calculated from Eq. (3) differs from accessible porosity, $\varepsilon_a(\text{orga})$. Thus, we used the parameter $\Pi(\text{orga})$ to extrapolate accessible porosity, assuming a similar correlation between exclusion factor and accessible porosity for both chloride and organic anions. This was achieved turning Eq. (8) into Eq. (9):

$$\varepsilon_a(\text{orga}) = \varepsilon(\text{water}) \times \Pi(\text{orga})^{1/m} \quad (9)$$

with $m = 1.6$ chosen for m-Archie's law. The experimental values $\Pi(\text{orga})$ and $\varepsilon(\text{water})$ were used to extrapolate $\varepsilon_a(\text{orga})$, and corresponding data were reported in Table 2. A wide range of exclusion was observed for these organic anions in COx clay rock, i.e. $0.03 < \varepsilon_a(\text{orga}) < 0.13$. The variability among accessible porosities may affect the retardation of organic anions, as discussed in section 4.2.

3.4. Diffusive Retardation of organic acids in clay rock

The Eq. (2) is usually used to model diffusion, assuming the following hypotheses: i) Adsorption only occurs of cations for which all the porosity is accessible, i.e. $\varepsilon(\text{cation}) = \varepsilon(\text{water})$, ii) Anions display a negligible adsorption and are partially excluded from porosity, i.e. $\varepsilon_a(\text{anion}) < \varepsilon(\text{water})$ and $R_d^{\text{APP}}(\text{anion}) = 0$. These hypotheses are questionable for oxoanions or organic anions (Frasca et al., 2014). It was shown previously that organic anions display both properties of adsorption ($R_d^{\text{APP}} > 0$) and of anion exclusion ($\Pi(\text{orga}) \ll 1$) in clay-rich media (Dagnelie et al., 2014; Chen et al., 2018). This study confirmed this affinity, with values $\alpha(\text{orga}) \gg \varepsilon_a(\text{orga})$ in most of the experiments (Table 2). The apparent porosity, $\alpha(\text{orga})$, allowed a quantification of adsorption averaged on the intact solid samples. The values from diffusion experiments, R_d^{CELL} , were calculated with Eq. (10), using $\alpha(\text{orga})$ and $\varepsilon_a(\text{orga})$ (extrapolated from $\Pi(\text{orga})$, see section 3.3):

$$R_d^{CELL} = \frac{(\alpha - \varepsilon_a)}{\rho_g(1 - \varepsilon)} \quad (10)$$

$$R_d^{BATCH} = \frac{1}{L} \int_{x=0}^L R_d\left(\frac{C_0 x}{L}\right) dx = \frac{Q}{C_0} \times \ln(1 + K_L \times C_0) \quad (11)$$

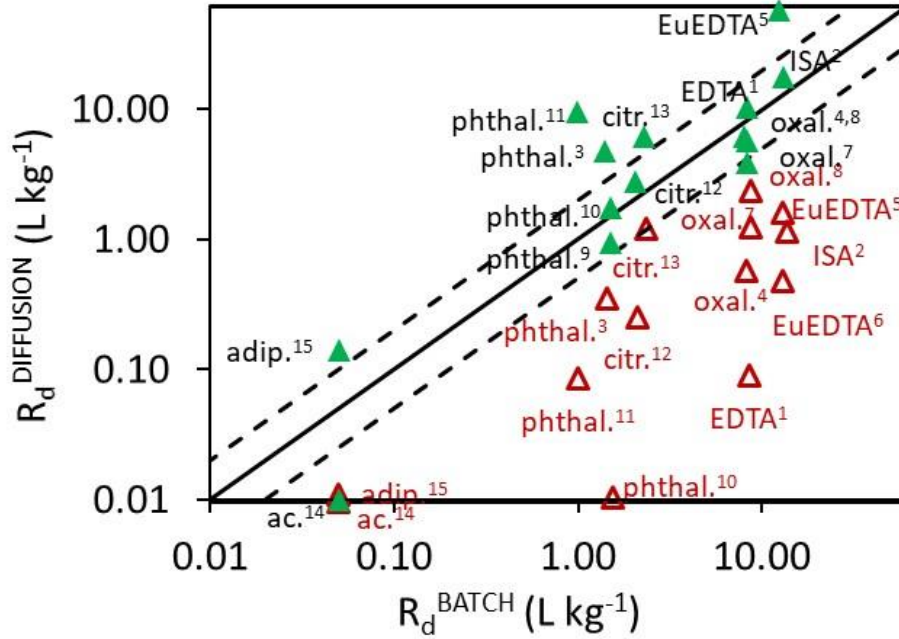


Figure 4: Solid-liquid distribution coefficients in batch and diffusion experiments.

X axis refers to the values from batch data and extrapolated to diffusion setup, R_d^{BATCH} . Y axis refers to values directly adjusted with the results of diffusion experiments. (Empty triangles): Apparent distribution coefficient calculated with Eq. (10), R_d^{CELL} . (Filled triangles) Corrected values extrapolated at infinite ionic strength with Eq. (12) (without exclusion), R_d^{CORR} . Superscripts indicate the number of the diffusion experiment.

Diffusion data, R_d^{CELL} were compared to batch data on crushed rock, R_d^{BATCH} , extrapolated to diffusion setup with Eq. (11). A linear profile of concentration was assumed along the diffusion pathway, $C(x) = C_0 \times [1 - x/L]$. Then the solid-liquid distribution coefficient was averaged on the solid sample using the Langmuir law, defined in Eq. (2): $R_d(C) = f(Q, K_L, C)$. This allowed us taking into account possible saturation effects expected during the diffusion experiment. For example, at low concentration in upstream reservoir ($C_0 \ll 1/K_L$), no saturation is expected in the solid sample and the solid-liquid

distribution coefficient reaches the value of the plateau of Langmuir isotherm: $R_d^{\text{BATCH}} \sim Q \times K_L$. While at high concentration in upstream reservoir ($C_0 \sim 1/K_L$), a saturation of sorption sites is expected, with a decrease of R_d^{BATCH} following Eq. (11). The comparison between adsorption in cells, expected from batch and diffusion data is reported in Fig. 4 (red empty symbols). A disagreement was observed, with an adsorption measured by diffusion experiment much lower than that expected from batch data. The origin and outcomes of these results are discussed below.

4. Discussion

The following discussion assesses the accuracy of the generalized law, Eq. (3), to predict migration of organic compounds. The validity of this approach is discussed with emphasis on retardation in various environmental media.

4.1. Diffusive retardation of organic molecules in various media

Sorption and retardation data are compared in Fig. 5 for organic compounds of various charges, structures and size. Data were represented as a function of hydrophilicity / lipophilicity of sorbates, quantified by the apparent octanol water partition coefficient which takes into account ionization of molecules (P_{app} (Sangster, 1989), detailed in supplementary material, Eq. (S1)).

The right part (red triangles) corresponds to absorption of lipophilic molecules by soil organic matter. The mechanism of absorption was evidenced by the emergence of a correlation after normalization by the content of natural organic matter, $[OC]$ ($K_{OC} = R_d / [OC]$). Data measured by diffusion experiment with lipophilic organic molecules on solid samples were added for comparison (red empty triangles, Vinsot et al., 2017). In this study, the out-diffusion of dissolved gas was monitored from Opalinus host rock during 8 years. A good agreement is obtained between data measured on crushed clay rock (batches) and intact host-rock (out-diffusion). The diffusive retardation is mainly driven by the lipophilicity of sorbate and the content of organic matter of the sorbent. The trend also evidence that the

contribution of soil organic matter to sorption becomes negligible compared to other sorbents at low lipophilicity ($\text{Log}(P_{\text{APP}}) \ll 1$).

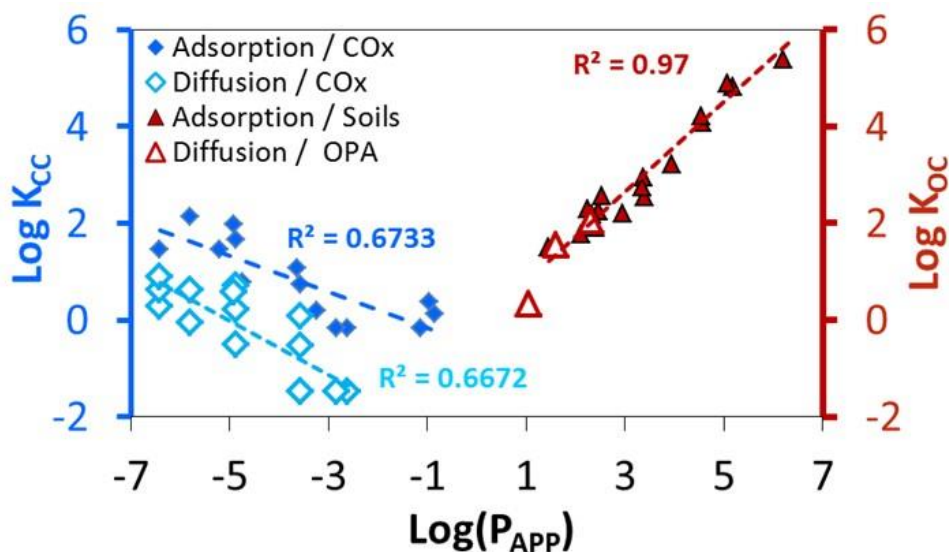


Figure 5: Comparison between batch and diffusion experimental results.

Right part (red): Absorption of lipophilic compounds in soil organic matter: $K_{OC} = R_d / [OC]$ (Organic Content).

(Filled triangles) Adsorption data on various soils. Taken from Karickhoff (1979); Chiou et al. (1979); Kenaga et al. (1978). (Empty triangles) Retardation data in Opalinus clay taken from Vinsot et al. (2017). Left part (blue):

Adsorption of hydrophilic anions. $K_{CC} = R_d / [CC]$ (Clay Content). (Filled squares) Adsorption on COx clay rock. Data taken from Rasamimanana et al. (2017a). (Empty squares) Diff. data in COx clay rock (this study).

The left part (blue filled squares) corresponds to adsorption of hydrophilic molecules in COx clay rock and data are taken from Rasamimanana et al., (2017a). Adsorption data are normalized by the clay content of the media [CC] ($K_{CC} = R_d / [CC]$). The negative slope of the correlation indicates that molecules with higher dipole moments display higher affinities for surfaces ($\text{Log}K_{CC} \nearrow$) but lower lipophilicity ($\text{log}P_{\text{APP}} \searrow$). For these systems, a mechanism of adsorption on mineral surfaces was proposed by Rasamimanana et al. (2017b). It was also evidenced that clay minerals are involved in adsorption of organic acids such as phthalate (Rasamimanana et al., 2017a). Diffusion data from our study were added in Fig. 5 (blue empty squares) for comparison with previous adsorption data. A low retardation ($K_{CC} > 0$)

was observed for organic molecules despite anion exclusion. Both adsorption and diffusion data displayed correlations ($R^2 \sim 0.67$) with hydrophilicity of diffusing molecules, $\text{Log}(P_{\text{APP}})$. Data in Fig. 5 still displayed some disparities because adsorption of anions depends on several factors such as charge, size, polarizability, or structure of sorbates (Kubicki et al., 1999).

A discrepancy was evidenced in Fig. 5 (blue squares) between data measured by adsorption in batch on crushed samples and adsorption calculated from diffusion experiments through solid intact samples. Similar discrepancy was already observed for organic acids / soils systems. For example, it is known that fluid percolation may induce a leaching of surfaces, leading to an increase of adsorption (Szecsody et al., 1994). Yet, it was surprising in our case that adsorption of carboxylates measured during diffusion was lower than that measured by batch experiments. Some possible processes involved are discussed in the following section.

4.2 Discrepancy between batch and diffusion data

The hypothesis of an apparent irreversibility of adsorption and or hydrodynamic of the system is sometimes given to discuss discrepancy between adsorption data measured on crushed and intact samples (Treumann et al., 2014). Durce et al. (2014) studied transport of polymaleic acid in COx clay rock using a two-sites irreversible sorption model. This model allowed replicating simultaneously desorption hysteresis in batch systems and percolation results. However, this hypothesis was ruled out in our study thanks to the use of through-diffusion experiments, leading to similar apparent porosities independently of sorption reversibility. Another possible hypothesis was a slow adsorption kinetics. For example, apolar organic molecules are absorbed by organic matter, with slow kinetics due to intra-particulate diffusion process (Pignatello and Xing, 1996). Yet, a fast kinetics was evidenced in the case of adsorption of organic acids in COx clay rock (Rasamimanana et al., 2017b). The hypothesis of slow adsorption kinetics seemed also unlikely, given the time-scale of diffusion experiments. A last hypothesis

was a modification of accessible surfaces due to exclusion of solutes from a part of porosity. Various modelling approaches were developed to describe effect of anion exclusion on accessible porosity (Bacle et al., 2016; Tournassat and Appelo, 2011; Wigger and Van Loon, 2017). Yet, most of these studies consider cations as sorbing species and anions as non-sorbing species. In the following section, we discuss the possible effect of exclusion of sorbing anions, accounting for a modification of diffusive retardation.

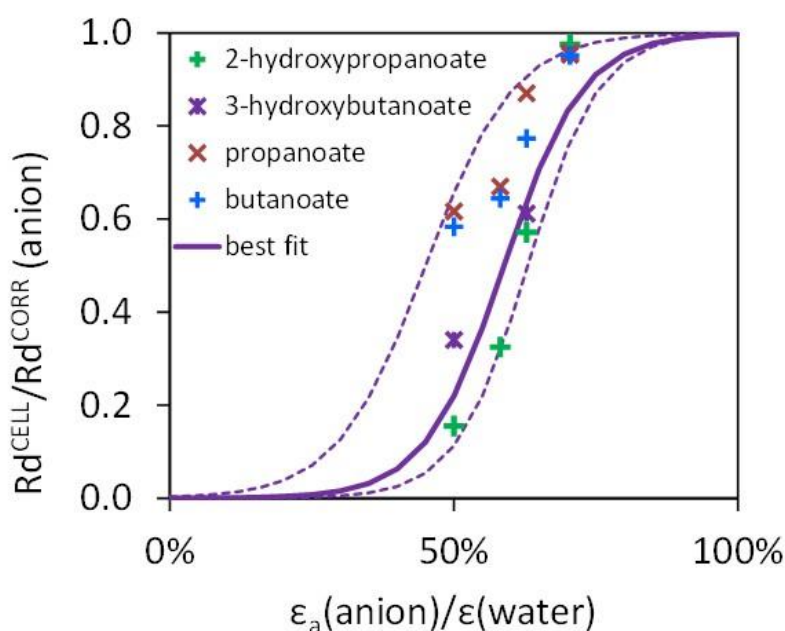


Figure 6: Adsorption of carboxylic acids, R_d^{CELL} (percolation through compacted illite).

Data taken from Chen et al. (2018). Data normalized by the value extrapolated at infinite ionic strength, R_d^{CORR} .

Values between brackets indicate ionic strength (in moles L^{-1}). Uncertainty ranges on best fit parameters represented by dashed lines.

The possible effect of anion exclusion on retardation was evaluated using data from Chen et al. (2018). These authors studied percolation of small organic anions in compacted illite. They observed a double effect of ionic strength, decreasing anion exclusion and increasing retardation, suggesting a link between retardation and anion exclusion. A maximum value of solid-liquid distribution coefficient was extrapolated at infinite ionic strength, R_d^{CORR} (detailed in Fig. S7, table S4). The ratio between measured

adsorption (R_d^{CELL}) and maximum adsorption (R_d^{CORR}) was defined as correction factor : f^{CORR} . Fig. 6 shows the corresponding correction factor as the function of accessible porosity. A correlation appeared between data with a Pearson correlation coefficient of 0.81 ± 0.16 . This correlation indicated a decrease of apparent distribution coefficient with anion exclusion: $R_d^{CELL}/R_d^{CORR} \rightarrow 0$ when $\varepsilon_a/\varepsilon \rightarrow 0$. Adsorption reached a maximum when there was no exclusion: $R_d^{CELL}/R_d^{CORR} \rightarrow 1$ when $\varepsilon_a/\varepsilon \rightarrow 1$. We choose the following 2-parameters logistic function to reproduce the shape of these experimental results:

$$f^{CORR} = \frac{R_d^{CORR}}{R_d^{CELL}} = \left[1 + \exp\left(a \times \left(b - \frac{\varepsilon_a}{\varepsilon}\right)\right) \right]^{-1} \quad (12)$$

The parameter “a” represents the steepness of the curve and the parameter “b” represents a threshold value of $\varepsilon_a/\varepsilon$. The best fit parameters obtained were $a = 14.4$ and $b = 0.59$ and corresponding curve was shown in Fig. 6 with associated uncertainty ranges: $a \in [13-16]$, $b \in [0.45-0.63]$. A similar correlation was assumed in compacted illite and COx clay rock. We calculated corrected values, R_d^{CORR} , for each organic compound using Eq. (12). The values are listed in Table 2 and compared to adsorption in batch in Fig. 4 (Green filled triangles). A relative agreement is observed between adsorption data and corrected diffusion data. The hypothesis of anion exclusion in intact samples leading to a reduced accessible porosity or surface seems plausible. The electrostatic nature of such effect was confirmed with oxalate data. An increase of ionic strength by a factor 5 between experiments n°7 and n°8, led to an increase of R_d^{CELL} by a factor two, from 1.3 to 2.3 L kg⁻¹.

Diffusion data suggested that surfaces accessible for organic anions differ between dispersed particles and solid intact samples. An increase of ionic strength led to strong variations of both anion exclusion and diffusive retardation (Chen et al., 2018; This work), but little effect on adsorption in batches (Rasamimanana et al., 2017a). The size of pores and surfaces involved in retardation are yet to be

characterized for organic anions. Clay-rich media display small micropores, including interlayer porosity (Gaboreau et al., 2016; Keller et al., 2011; Song et al., 2015). Anions are supposed to be excluded from interlayer porosity (Bacle et al., 2016; Tournassat et al., 2011; Van Loon et al., 2007), but anion exclusion is not only depending on pore size distribution (Tournassat et al., 2016; Wigger and Van Loon, 2017). Further studies of these systems would be necessary, with a better description of clay sample, including characterization of pore-size distribution, pore shape, and surfaces interacting with organic sorbates.

5. Conclusion

In this study we evaluated through-diffusion of organic anions through the Callovo-Oxfordian clay-rich rock. Low effective diffusion coefficients were measured for organic compounds, with D_e values ranging between 0.5 and $7 \cdot 10^{-12} \text{ m}^2 \text{ s}^{-1}$. These values quantified the exclusion of organic anions from rock porosity, due to both charges and size effects. Effective diffusion coefficients were useful to evaluate the accessible porosities of organic anions. This was made using an empirical m-Archie's law. The calculated accessible porosities of organic anions were 30% to 80% lower than that of water.

Despite anion exclusion, some affinity of organic anions for rock surfaces was evidenced and quantified by diffusive retardation. Diffusion experiments indicated much lower adsorption values than expected from measurements on dispersed systems (batches). Several hypotheses may explain these differences between crushed and solid samples, e.g. role of minor phases, slow evolution of speciation or oxydoreduction. We discussed the specific hypothesis of a correlation between anion exclusion and retardation, given their dependency with ionic strength. The decrease of accessible porosity for a diffusing solute was supposed to reduce the accessibility to surfaces, thus leading to a reduced retardation. An empirical correction factor was proposed to quantify the reduced retardation with a threshold value of accessible porosity under which the retardation significantly decreases. Using this correction factor, a reasonable agreement was observed between adsorption experiments in batches and diffusion experiments in cell. The retardation factor was negligible for the most excluded species, i.e. with values $\varepsilon_a/\varepsilon \ll 0.59$,

meaning $D_e \ll 2 \cdot 10^{-12} \text{ m}^2 \text{ s}^{-1}$. Still, a significant retardation was observed for several species: e.g. oxalate, ETDA or ISA.

Nevertheless, it seems necessary to measure retardation factors of organic anions by transport experiments in sedimentary rocks, rather than performing extrapolation from adsorption in batch studies. Similar behaviour may arise in other materials with charged surfaces such as cementitious materials or oxisoils. It would be interesting to compare several media, since the solutes affinity or exclusion will differ from one media to another.

Acknowledgments

In memory of Dr. Eric Giffaut. This work was partially financed by the National Radioactive Waste Management Agency (Andra). We thank F. Goutelard for early diffusive experiments at various ionic strengths. We thank four anonymous reviewers, Dr. S. Savoye and A. Rajyaguru for time consuming reading and many constructive comments.

References

- Altmann, S., Tournassat, C., Goutelard, F., Parneix, J.-C., Gimmi, T., Maes, N. 2012. Diffusion-driven transport in clayrock formations. *Applied Geochem.* 27, 436–478.
- Archie, G.E., 1942. The electrical resistivity log as an aid in determining some reservoir characteristics. *Trans. AIME* 146, 54–62.
- Bacle, P., Dufrêche, J.-F., Rotenberg, B., Bourg, I.C., Marry, V. 2016. Modeling the transport of water and ionic tracers in a micrometric clay sample. *Appl. Clay Sci.* 123, 18–28.
- Bazer-bachi, F., Tevissen, E., Descostes, M., Grenut, B., Meier, P., Simonnot, M., Sardin, M., 2006. Characterization of iodide retention on Callovo-Oxfordian argillites and its influence on iodide migration. *Phys. Chem. Earth, Parts A/B/C* 31, 517–522.
- Bazer-Bachi, F., Descostes, M., Tevissen, E., Meier, P., Grenut, B., Simonnot, M.-O., Sardin, M., 2007. Characterization of sulphate sorption on Callovo-Oxfordian argillites by batch, column and through-diffusion experiments, *Physics and Chemistry of the Earth, Parts A/B/C*, 32, 8–14.
- Borisover, M., Graber, E.R., 1997. Specific interaction of Organic compounds with soil organic carbon. *Chemosphere* 34, 8, 1761–1776.
- Borisover, M., Davis, J., 2015. Adsorption of inorganic and organic solutes by clay minerals. in: Tournassat, C., Steefel, C., Bourg, I.C., Bergaya, F. (Eds.), *Natural and Engineered Clay Barriers*. Elsevier.
- Brusseau, M.L., 1991. Nonequilibrium Sorption of Organic Chemicals: Elucidation of Rate-Limiting Processes. *Environ. Sci. Technol.* 25, 134–142.
- Charlet, L., Alt-Epping, P., Wersin, P., Gilbert, B., 2017. Diffusive transport and reaction in clay rocks: A storage (nuclear waste, CO₂, H₂), energy (shale gas) and water quality issue. *Adv. Water Res.* 106, 39–59.
- Chen, Y., Glaus, M.A., Van Loon, L.R., Mäder, U., 2018. Transport of low molecular weight organic compounds in compacted illite and kaolinite. *Chemosphere* 198, 226–237.
- Chiou, C.T., Peters, L.J., Freed, V.H., 1979. A physical concept of soil-water equilibria for nonionic organic compounds. *Science* 80 (206), 831–832.
- Crank, J., 1975. *The Mathematics of Diffusion*. Clarendon Press, London.
- Curtis, G.P., Roberts, P.V., Reinhard, M. 1986. A Natural Gradient Experiment on Solute Transport in a Sand Aquifer. Sorption of Organic Solutes and its Influence on Mobility. *Wat. Res. Research* 22, 13, 2059–2067.

Dagnelie, R.V.H., Descostes, M., Pointeau, I., Klein, J., Grenut, B., Radwan, J., Lebeau, D., Geogin, D., Giffaut, E., 2014. Sorption and diffusion of organic acids through clayrock: comparison with inorganic anions. *J. Hydrol.* 511, 619–627.

Dagnelie, R.V.H., Arnoux, P., Radwan, J., Lebeau, D., Nerfie, P., Beaucaire, C., 2015. Perturbation induced by EDTA on HDO, Br⁻ and Eu^{III} diffusion in a large-scale clay rock sample. *Appl. Clay Sci.* 105–106, 142–149.

Dagnelie, R.V.H., Arnoux, P., Enaux, J., Radwan, J., Nerfie, P., Page, J., Coelho, D., Robinet, J.-C., 2017. Perturbation induced by a nitrate plume on diffusion of solutes in a large-scale clay rock sample. *Appl. Clay Sci.* 141, 219–226.

Delage, P., Cui, Y.J., Tang, M., 2010. Clays in radioactive waste disposal. *J. Rock. Mech. And Geotech. Eng.* 2 (2), 111–123.

Descostes, M., Blin, V., Bazer-Bachi, F., Meier, P., Grenut, B., Radwan, J., Schlegel, M.L.,

Buschaert, S., Coelho, D., Tevissen, E., 2008. Diffusion of anionic species in Callovo-Oxfordian argillites and oxfordian limestones (Meuse/Haute-Marne, France). *Appl. Geochem.* 23, 655–677.

Descostes, M., Pointeau, I., Radwan, J., Poonoosamy, J., Lacour, J.-L., Menut, D., Vercouter, T., Dagnelie, R.V.H., 2017. Adsorption and retarded diffusion of Eu^{III}-EDTA⁻ through hard clay rock. *J. Hydrol.* 544, 125–132.

Duarte, R., Matos, J., Senesi, N., 2018. Chapter 5 - Organic Pollutants in Soils, In *Soil Pollution*, edited by A. C. Duarte, A. Cachada and T. Rocha-Santos, Academic Press, 103–126.

Durce, D., Landesman, C., Grambow, B., Ribet, S., Giffaut, E., 2014. Adsorption and transport of polymaleic acid on Callovo-Oxfordian clay stone: batch and transport experiments. *J. Contam. Hydrol.* 164, 308–322.

Frasca, B., Savoye, S., Wittebroodt, C., Leupin, O.X., Descostes, M., Grenut, B., Etep-Batanken, J., Michelot, J.-L., 2012. Influence of redox conditions on iodide migration through a deep clay formation (Toarcian argillaceous rock, Tournemire, France). *Appl. Geochem.* 27, 2456–2462.

Frasca, B., Savoye, S., Wittebroodt, C., Leupin, O.X., Michelot, J.-L., 2014. Comparative study of Se oxyanions retention on three argillaceous rocks: Upper Toarcian (Tournemire, France), Black Shales (Tournemire, France) and Opalinus Clay (Mont Terri, Switzerland). *J. Environ. Rad.* 127, 133–140.

Furukawa, K.; Takahashi, Y.; Sato, H. 2007. Effect of the formation of EDTA complexes on

- the diffusion of metal ions in water. *Geochim. Cosmochim. Acta* 71, 4416–4424.
- Gaboreau, S., Robinet, J.-C., Prêt, D., 2016. Optimization of pore-network characterization of a compacted clay material by TEM and FIB/SEM imaging. *Microp. Mesopo. Materials* 224, 116–128.
- Gaucher, E., Robelin, C., Matray, J., Negrel, G., Gros, Y., Heitz, J., Vinsot, A., Rebours, H., Cassagnabère, A., Bouchet, A., 2004. ANDRA underground research laboratory: interpretation of the mineralogical and geochemical data acquired in the Callovo-Oxfordian formation by investigative drilling. *Phys. Chem. Earth* 29, 55–77.
- Gu, B., Mehlhorn, T.L., Liang, L., McCarthy, J.F., 1996. Competitive adsorption, displacement, and transport of organic matter on iron oxide: I. Competitive adsorption. *Geochim. Cosmochim. Acta* 60, 1943–1950.
- Hansch, C. Leao, A., Hoekman, D., 1995. Exploring QSAR – Hydrophobic, Electronic and Steric Constants. American Chemical Society, Washington, DC, p. 38.
- Hummel, W., 2008. Radioactive contaminants in the subsurface: the influence of complexing ligands on trace metal speciation. *Monatshefte für Chemie - Chem. Mon.* 139, 459–480.
- Jacquier, P., Hainos, D., Robinet, J.-C., Herbette, M., Grenut, B., Bouchet, A., Ferry, C., 2013. The influence of mineral variability of Callovo-Oxfordian clay rocks on radionuclide transfer properties. *Applied Clay Sci.* 83–84, 129–136.
- Jardine, P.M., Weber, N.L., McCarthy, J.F., 1989. Mechanisms of dissolved organic carbon adsorption on soil. *Soil Sci. Soc. Am. J.* 53, 1378–1385.
- Karickhoff, S.W., Brown, D.S., Scott, T.A., 1979. Sorption of Hydrophobic Pollutants on Natural Sediments. *Wat. Res.* 13, 241–248.
- Keller, L.M., Holzer, L., Wepf, R., Gasser, P. 2011. 3D Geometry and topology of pore pathways in Opalinus clay: Implications for mass transport. *Applied Clay Sci.* 52, 85–95.
- Kenaga, E.E., Goring, C.A.I. 1978. Relationship between water solubility, soil sorption, octanol-water partitioning and bioconcentration of chemicals in biota. *Proc. 3rd Symp. Aquat. Toxic.* 678–715.
- Kubicki, J.D., Schroeter, L.M., Itoh, M.J., NGuyen, B.N., Apitz, S.E., 1999. Attenuated total reflectance Fourier-transform infrared spectroscopy of carboxylic acids adsorbed onto mineral surfaces. *Geochim. Cosmochim. Acta* 63, 2709–2725.
- Lerouge, C., Grangeon, S., Gaucher, E.C., Tournassat, C., Agrinier, P., Guerrot, C., Widory, D., Fléhoc, C., Wille, G., Ramboz, C., Vinsot, A., Buschaert, S., 2011. Mineralogical and isotopic record of biotic and abiotic diagenesis

of the Callovo-Oxfordian clayey formation of Bure (France). *Geochim. Cosmochim. Acta* 75 (10), 2633–2663.

Liu, H., Chen, T., Frost, R.L., 2014. An overview of the role of goethite surfaces in the environment. *Chemosphere* 103, 1–11.

Melkior, T., Yahiaoui, S., Thoby, D., Motellier, S., Barthes, V., 2007. Diffusion coefficients of alkaline cations in Bure mudrock. *Phys. Chem. Earth Parts A/B/C* 32, 453–462.

Montavon, G., Sabatié-Gogova, A., Ribet, S., Bailly, C., Bessaguet, N., Durce, D., Giffaut, E., Landesman, C., Grambow, B., 2014. Retention of iodide by the Callovo-Oxfordian formation: An experimental study. *Appl. Clay Sci.* 87, 142–149.

Mika, E.T.S., Kurinawan, T.A., Lo, W.H., 2011. Degradation of chelating agents in aqueous solution using advanced oxidation process (AOP). *Chemosphere* 83, 1443–1460.

Moridis, G.J., 1998. A Set of semianalytical solutions for parameter estimation in diffusion cell experiments. *Sci. York*.

Nowack, B., Xue, H., Sigg, L., 1997. Influence of Natural and Anthropogenic Ligands on Metal Transport during Infiltration of River Water to Groundwater. *Environ. Sci. Technol.* 31, 866–872.

Pellenard, P., Deconinck, J.-F., 2014. Mineralogical variability of callovo-oxfordian clays from the Paris basin and the subalpine basin. *C.R. Geosci.* 338, 854–866.

Pignatello, J.J., Xing, B., 1996. Mechanisms of Slow Sorption of Organic Chemicals to Natural Particles. *Environ. Sci. Technol.* 30, 1, 1–11.

Pinsuwan, S., Li, L., Yalkowsky, S.H., 1995. Correlation of octanol/water solubility ratios and partition coefficients. *J. Chem. Eng. Data* 40, 623.

Rasamimanana, S., Lefèvre, G., Dagnelie, R., 2017a. Adsorption of polar organic molecules on sediments : Case-study on Callovian-Oxfordian claystone. *Chemosphere* 181, 296–303.

Rasamimanana, S., Lefèvre, G., Dagnelie, R., 2017b. Various causes behind desorption hysteresis of carboxylic acids on mudstones. *Chemosphere* 168, 559–567.

Read, D., Ross, D., Sims, R.J., 1998. The migration of uranium through Clashach Sandstone: the role of low molecular weight organics in enhancing radionuclide transport. *J. Contam. Hydrol.* 35, 235–248.

Ribeiro, A.C.F., Rita, M.B.B.J., Gomes, J.C.S., Lobo, V.M.M., Estes, M.A. 2011. Diffusion of calcium gluconate in aqueous solutions of lactose at 298.15K. *Food Chem.* 126, 1186–1189.

Roberts, P.V., Goltz, M.N., Mackay, D.M., 1986. A Natural Gradient Experiment on Solute Transport in a Sand Aquifer 3. Retardation Estimates and Mass Balances for Organic Solutes. *Wat. Res. Research* 22, 13, 2047–2058.

Rosanne, M., Mammari, N., Koudina, N., Prunet-Foch, B., Thovert, J.-F., Tevissen, E., Adler, P.M. 2003. Transport properties of compact clays II. Diffusion. *J. Colloid Interface Sci.* 260, 195–203.

Roy, S.B., Dzombak, D.A. 1998. Sorption nonequilibrium effects on colloid-enhanced transport of hydrophobic organic compounds in porous media. *J. Contam. Hydrol.* 30, 179–200.

Sangster, J., 1989. Octanol-water partition coefficient of simple organic compounds. *J. Phys. Chem. Ref. Data* 18 (3), 1111–1227.

Savoie, S., Goutelard, F., Beaucaire, C., Charles, Y., Fayette, A., Herbette, M., Larabi, Y., Coelho, D., 2011. Effect of temperature on the containment properties of argillaceous rocks:

The case study of Callovo–Oxfordian claystones. *J. Contam. Hydrol.* 125, 102–112.

Savoie, S., Beaucaire, C., Fayette, A., Herbette, M., Coelho, D., 2012a. Mobility of cesium through the Callovo–Oxfordian claystones under partially saturated conditions. *Environ. Sci. Technol.* 46, 2633–2641.

Savoie, S., Frasca, B., Grenut, B., Fayette, A., 2012b. How mobile is iodide in the Callovo–Oxfordian claystones under experimental conditions close to the in situ ones?, *J. Contam. Hydrol.* 142–143, 82–92.

Savoie, S., Beaucaire, C., Grenut, B., Fayette, A., 2015. Impact of the solution ionic strength on strontium diffusion through the Callovo–Oxfordian clayrocks: an experimental and modelling study. *Appl. Geochem.* 61, 41–52.

Schaffer, M., Licha, T., 2015. A framework for assessing the retardation of molecules in groundwater: Implications of the species distribution for the sorption-influenced transport. *Sci. Total Environ.* 524–525, 187–194.

Shackelford, C.D., Moore, S.M. 2013. Fickian diffusion of radionuclides for engineered containment barriers: Diffusion coefficients, porosities, and complicating issues. *Engineering Geol.* 152, 133–147.

Song, Y., Davy, C., Troadec, D., Blanchenet, A.-M., Skoczylas, F., Talandier, J., Robinet, J.-C. 2015. Multi-scale pore structure of COx claystone: Towards the prediction of fluid transport. *Mar. Pet. Geol.* 65, 63–82.

Szecsody, J.E., Zachara, J.M., Bruckhart, P.L., 1994. Adsorption-Dissolution Reactions Affecting the Distribution and Stability of Co^{II}EDTA in Iron Oxide-Coated Sand. *Environ. Sci. Technol.* 28, 1706–1716.

Szecsody, J.E., Zachara, J.M., Chilakapati, A., Jardine, P.M., Ferency, A.S., 1998. Importance of flow and particle-scale heterogeneity on Co^{II/III} EDTA reactive transport. *J. Hydrol.* 209, 112–136.

Tournassat, C., Appelo, C.A.J. 2011. Modelling approaches for anion-exclusion in compacted Na-bentonite. *Geochim. Cosmochim. Acta* 75, 3698–3710.

Tournassat, C., Steefel, C. I., Bourg, I. C., Bergaya, F. Editor(s), Natural and Engineered Clay Barriers, In *Developments in Clay Science*, Elsevier, 2015. 6, 1572–4352.

Tournassat, C., Gaboreau, S., Robinet, J.-C., Bourg, I., Steefel, C.I. 2016. Impact of microstructure on anion exclusion in compacted clay media. *The Clays Minerals Society Workshop Lectures Series*, 21, 11, 137–149.

Treumann, S., Torkzaban, S., Bradford, S., Visalakshan, R.M., Page, D. 2014. An explanation of differences in the process of colloid adsorption in batch and column studies. *J. Contam. Hydrol.* 164, 219–229.

Van Brakel, J., Heertjes, P.M., 1974. Analysis of diffusion in macroporous media in terms of a porosity, a tortuosity, and a constrictivity factor. *J. Heat Mass Transfer* 17, 1093–1103.

Van Loon, L.R., Glaus, M., Müller, W., 2007. Anion exclusion effects in compacted bentonites: Towards a better understanding of anion diffusion. *Applied Geochem.* 22, 2536–2552.

Van Loon, L.R., Mibus, J., 2015. A modified version of Archie's law to estimate effective diffusion coefficients of radionuclides in argillaceous rocks and its application in safety analysis studies. *Applied Geochem.* 59, 85–94.

Vinsot, A., Anthony, C., Appelo, J., Lundy, M., Wechner, S., Cailteau-Fischbach, C., de Donato, P., Pironon, J., Lettry, Y., Lerouge, C., De Cannière, P., 2017. Natural gas extraction and artificial gas injection experiments in Opalinus Clay, Mont Terri rock laboratory (Switzerland). *Swiss J. Geosci.* 110, 375–390.

Wang, Y., Liu, H., Peng, Y., Tong, L., Feng, L., Ma, K. (2018) New pathway for the biodegradation of diethyl phthalate by *Sphingobium yanoikuyae* SHJ. *Proc. Biochem.* 71, 152–158.

Weber, W.J.Jr., McGinley, P.M., Katz, L.E. 1991. Sorption phenomena in subsurface systems: concepts, models and effects on contaminant fate and transport. *Wat. Res.* 25, 5, 499–528.

Wigger, C., Van Loon, L.R., 2017. Importance of interlayer equivalent pores for anion diffusion in clay-rich sedimentary rocks. *Environ. Sci. Technol.* 51 (4), 1998–2006.

Wigger, C., Gimmi, T., Muller, A., Van Loon, L.R., 2018. The influence of small pores on the anion transport properties of natural argillaceous rocks – A pore size distribution investigation of Opalinus Clay and Helvetic Marl. *Applied Clay Sci.* 156, 134–143.

Zachara, J.M., Gassman, P.L., Smith, S.C., Taylor, D., 1995. Oxidation and adsorption of Co(II) EDTA₂ complexes in subsurface materials with iron and manganese oxide grain coatings. *Geochim. Cosmochim. Acta* 59, 4449–4463.

Dagnelie et al., 2018 - Preprint version – Published version available in Chemosphere